In: 2010 IEEE International Conference on Robotics and Automation, Anchorage Convention District, May 3-8, 2010, Anchorage, Alaska, USA, pp 2598-2603

Novel Miniature MRI-Compatible Fiber-Optic Force Sensor for Cardiac Catherisation Procedures

Panagiotis Polygerinos, *Student Member, IEEE,* Pinyo Puangmali, Lakmal D. Seneviratne, *Member, IEEE* and Kaspar Althoefer, *Member, IEEE*

***Abstract*— This paper presents the prototype design and development of a miniature MRI-compatible fiber optic force sensor suitable for the detection of forces during cardiac catheterization. The working principle is based on light intensity modulation where a fiber optic cable interrogates a reflective surface at a predefined distance inside a catheter shaft. When a force is applied to the tip of the catheter, a force sensitive structure, which connects the tip with the rest of the catheter, reduces the distance between optical fiber and reflective surface or rotates the reflective surface against the fixed fiber. In both cases the light is modulated accordingly and the axial or lateral force can be estimated. The developed prototype passed preliminary experiments successfully. The sensor exhibits adequate linear response, having a good working range, very good resolution and good sensitivity in both axial and lateral force directions. In addition, the use of low-cost and MRI compatible materials for its development makes the sensor safe for use inside MRI environments.**

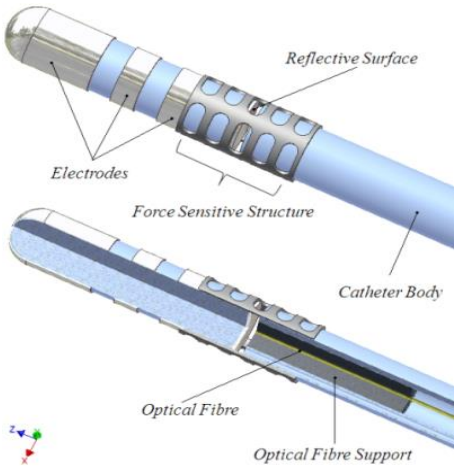

Fig. 1. CAD drawings of a 7 Fr. catheter integrated with the proposed fiber-optic force sensor.

I. Introduction

PERCUTANEOUS coronary interventions (PCI) and electrophysiology (EP) are minimally invasive procedures of the heart that are nowadays performed along existing routes inside the human body, such as blood vessels, and are carried out with the use of catheters. A catheter is a thin and flexible elongated tube that is inserted through a small incision in the groin (upper thigh), the arm, or the neck of the patient [1], where one of the main blood arteries is located. Catheter diameters are usually measured in French (Fr) which is one third of a millimetre.

During a cardiac catheterisation procedure the physician intents to reach certain locations via the blood vessels and perform examinations or offer treatment to tissues of the heart otherwise requiring open surgery. This is a Minimally Invasive Surgery (MIS) procedure that has to offer many advantages, including reduced trauma to tissues, reduced recovery time, less infections and lower overall hospitalisation costs [2].

A delicate procedure such as cardiac catheterisation relies on the doctor's experience in order to perform it in an accurate and safe way. At the moment, physicians make use of imaging techniques, such as X-ray fluoroscopy and Computed Tomography (CT) to navigate the catheters through the patient's body. These two techniques involve the use of an X-ray source and a detector to obtain real-time images of the internal structures of the patient. The images are taken in a sequence that can be showed to doctors in the form of a movie. In this way the internal body structures can be shown on the physicians monitor in real-time. From these techniques two-dimensional images are obtained, which can either show the skeletal structure (radiographic image), or the vasculature (angiogram) of the patient.

It is noted that fluoroscopy and CT employ ionizing technology to visualize the inner human structure. The use of X-rays makes them hazardous for the patients and the medical staff that performs the PCI or EP procedure. This time limits surgical procedures due to the risks of prolonged exposure to ionizing radiation. Furthermore, the quality of the returned tissue and organ images is poor; X-ray is more applicable to represent the skeletal structure of the human body. In addition, a contrast agent needs to be injected into the blood vessels or the heart in order to improve the visual ability. In large amounts that contrast agent can cause kidney failure and therefore is avoided as much as possible.

The above drawbacks have recently forced scientists to start looking for alternative imaging methods to perform cardiac catheterizations [3],[4]. One of the new methods that can provide distinct advantages over fluoroscopy and CT is Magnetic Resonance Imaging (MRI). MRI scanners operate with strong magnetic fields used to examine human networks of blood vessels and soft tissues without the need

Manuscript received August 18, 2009. Novel Miniature MRI-Compatible Fiber-Optic Force Sensor for Cardiac Catherisation Procedures

Panagiotis Polygerinos, Pinyo Puangmali, Lakmal D. Seneviratne, and Kaspar Althoefer are with King's College London, Department of Mechanical Engineering, Strand, London, WC2R 2LS, UK (email: panagiotis.polygerinos@kcl.ac.uk; pinyo.puangmali@kcl.ac.uk; lakmal.seneviratne@kcl.ac.uk; kaspar.althoefer@kcl.ac.uk).

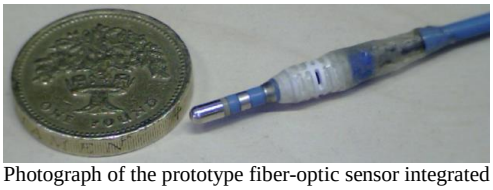

Fig. 2. Photograph of the prototype fiber-optic sensor integrated with a 7 Fr catheter. A one GB pound coin is shown for comparison.

for a contrast agent, producing three dimensional digital images of superior quality and most importantly without emitting hazardous ionizing radiations.

However, MRI scanners encompass a main constrain. Due to the high magnetic fields that are produced, the use of tools and instruments which contain materials that could affect the homogeneity of the magnetic field must be avoided inside the area of operation. Placing conductive wires inside an MRI scanner while in operation can potentially turn the wires into MR-antennas, possibly resulting in heating effects at the tip of the wire. Metal materials cannot be used as they either distort the MRI images, producing artefacts or due to the heating-up effects putting the life of patients at risk [5]. Thus, any material used must not increase the signal-to-noise ratio and must be magnetically inert and MRI safe [6].

In this paper a new prototype miniature catheter-tip force sensor that employs fiber-optic technology is presented. The intention is to bridge the gap between the detection of contact forces from the tissue-catheter interaction during a cardiac catheterization and the need of MRI-compatible sensors with low manufacturing cost.

II. Force Feedback in Cardiac Catheters

Any type of force feedback during the catheterisation procedure would aid the physician in achieving a better and faster outcome in the majority of cases. Interventional cardiologists are often able to sense the interaction of the catheter with the internal structures (e.g. blood vessels and atrium of the heart) while performing a catheterization. This haptic feedback is often used by the physician to determine the position of the catheter and facilitate the maneuvering of the catheter. The force feedback from the catheter also indicates, particularly in the case of an EP ablation, the outcome of the procedure, as a good contact of the catheter-tip assures a successful result. However, distinguishing between involved force components is a difficult task and requires extensive training from the side of the physician to achieve adequate expertise. The difficulty stems from the fact that the forces involved are a combination of two force components: one originates from the friction between the catheter and the blood vessels and the other from the catheter tip when in contact with the blood vessel or cardiac walls [7]. In addition, the orientation of the catheter-tip is independent and difficult to predict making any given task even more complicated.

Many types of force and pressure sensors have been developed in the past for use in catheterisation procedures. These sensors were used for different kinds of measurements, such as blood pressure, oxygen level, blood flow, blood velocity and others. They make use of several sensing principles, such as strain-gauges [8], piezoresistivity [9], PVDF films [1] and fiber-optic technology [10],[11]. However, only a small number of sensors were developed, for the detection of interaction contact forces between catheter and tissue [12], [13].

III. Novel Fiber-Optic Force Sensor

A. Prototype Sensor

For this research, a plastic 7 Fr catheter was used and divided in two parts (fig. 1). The first part, the tip of the catheter, accommodates the electrodes for EP ablation and a reflective flat circular face. The occupied area of the reflective surface is equal with the catheter's cross section and is located at the opposite end of the main tip electrode. The second part is the actual flexible shaft of the catheter. The two separate parts of the catheter are connected, positioned and aligned together with a force sensitive (deformable) structure of 12 Fr, allowing a very small gap of 0.6 mm to form between them. The main shaft contains a 0.25 mm in diameter plastic optical-fiber. The optical-fiber is held in position in such a way that the one end is at the same plane level where the end of the main catheter's shaft is. The remaining other end of the optical-fiber is connected with a photodiode detector.

With this configuration a light is emitted from a light source through the optical fiber onto a reflective surface and then reflected back to a photodiode. When a force is applied at the tip of the catheter, the connecting structure is deformed and modulating the light intensity that can be read out by the photodiode via an optical coupler and interpreted as a force signal.

B. Light Intensity Modulation

The principle of operation of the proposed force sensor is based on the variation of the light intensity caused by the change of height *h* (fig. 3 - Axial Force Loading) or rotation Θ (fig. 4 – Lateral Force Loading) of the reflective surface and the optical-fiber end. In both cases the light is transmitted and received through the same optical fiber.

A Gaussian curve can describe the light intensity distribution profile of the light beam. The value of the beam's intensity is a function described by the cross sectional radius of the beam. Therefore, assuming the optical fiber is a single mode fiber the light intensity distribution profile can be expressed in polar coordinates as

$$I_{(r)} = I_o e^{\left(-\frac{2r^2}{w_0^2}\right)}, \quad (1)$$

where $I_{(r)}$ is the current value of the beam's intensity at a radius r, I_o is the maximum intensity at radius r=0 and w_0 is t he mode-field radius; thus, mode-field diameter is equal to $2w_0$.

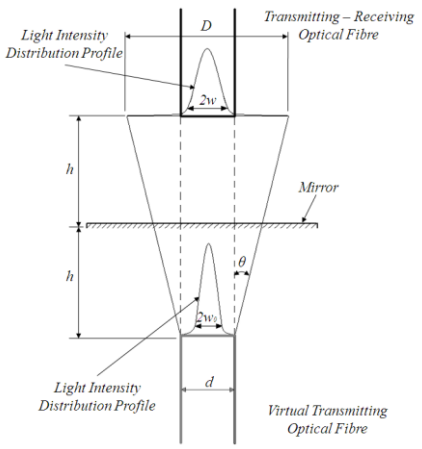

Fig. 3. Geometry of the light intensity modulation in the case of axial force loading of the sensor.

As a Gaussian curve has no boundaries and theoretically the light continues spreading to infinity, it is assumed that a boundary exists where the mode-field diameter is, (i.e. radius r of the cross section is equal to w_0). Substituting in equation (1) and assuming a relative intensity of 1, a drop of light intensity to $\frac{1}{e^2} = 0.135$ from the peak value is expected.

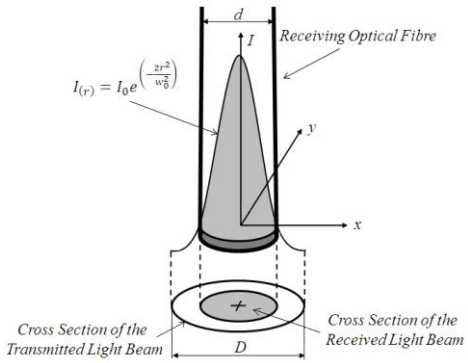

Fig. 4. Maximal transmitted light flux and the actual collected light flux that is bounded by the cross section of the optical fiber with diameter *d*.

Now that the boundaries have been defined the total flux of light can be estimated. Thus, the total transmitted light flux can be expressed as

$$\Phi_{tran.} = \int_0^{\frac{D}{2}} I_{(r)} 2\pi r dr \approx \int_0^{\infty} I_{(r)} 2\pi r dr = \frac{I_o \pi D^2}{4}, \quad (2)$$

where $\Phi_{tran.}$ is the total light flux which is transmitted from the optical fiber, D is the diameter of the cross sectional plane of the light flux at maximum distance from the optical fiber end and $I_{(r)}$ is the current value of the beam's intensity at radius r.

1) Axial Force Loading

In the case of axial sensor loading the optical fiber is facing the reflective surface vertically. The reflected light is received by the same optical fiber in a perpendicular manner in relation to the reflective surface. Any axial applied force reduces distance h between optical fiber and reflective surface (fig. 3). Therefore, to derive the equation of the collected light flux it is imperative to know the geometry of the light when it reflects at the surface.

Fig. 3 shows that light intensity I drops as the distance h increases, but the amount of light flux remains always the same. The change of the light intensity affects only the mode-field diameter. As a consequence, it must be noted that the total light flux received by the optical fiber is not the maximum emitted light flux at a distance h but, it is the flux bounded by the circular cross section of the receiving optical fiber with diameter d, see fig. 4. The following equation derives the maximal light flux able to be received by the optical fiber with w indicating the mode-field radius at the receiving fiber,

$$\Phi_{r,max} = \int_0^{\frac{d}{2}} I_{(r)} 2\pi r dr = \frac{I_o \pi w^2 \left(1 - e^{-\frac{d^2}{2w^2}}\right)}{2}. \quad (3)$$

Depending on the distance of the optical fiber from the reflective surface, the received light flux can vary and consequently the voltage output from the photo detector varies, too. The maximum voltage output that can be detected from the photo detector is given by

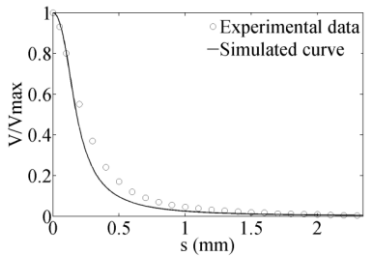

Fig. 5. Axial motion of optical fiber against a reflective surface: experimental data and simulation results (Eq. 5). The maximum error is 4.8%

$$V_{max} = k_v \sigma_r \int_0^{\frac{d}{2}} I_{(r)} 2\pi r dr = \frac{k_v \sigma_r I_0 \pi w^2 \left(1 - e^{-\frac{d^2}{2w^2}}\right)}{2} \quad (4)$$

where k_v transforms the received total flux of the detector into electrical signal and σ_r is the factor that compensates the losses during the receiving of the light from the detector. These losses originate from optical fiber misalignments at the connecting points within the force sensor housing and from optical fiber bending.

The normalized voltage output is computed from the ratio of the voltage output with the maximal voltage output that can be detected by the photo detector.

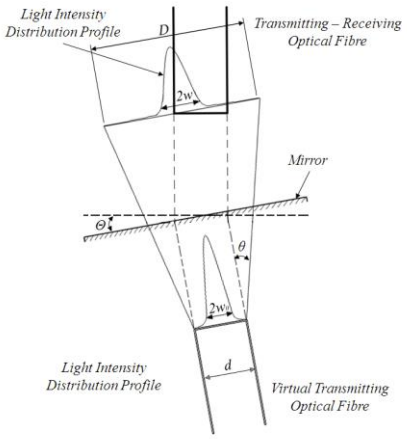

Fig. 6. Geometry of the light intensity modulation in the case of lateral force loading of the sensor. Amounts of light scatter away of the optical fiber boundaries.

$$\frac{V_{out}}{V_{max}} = \frac{w^2\left(1 - e^{-\frac{d^2}{2w^2}}\right)}{max\left[w^2\left(1 - e^{-\frac{d^2}{2w^2}}\right)\right]} \quad (5)$$

To validate the mathematical equations a test rig was set-up. The test rig consisted of a linear translational stage, a reflective surface (mirror) and a plastic optical fiber with a diameter of 0.25 mm and a core refractive index of 1.492 and a 61° light angle (θ = 30.5°). The test rig allows varying the distance between the mirror and the tip of the optic fiber whose longitudinal axis is kept perpendicular with respect to the mirror.

The experiment was conducted three times and the starting distance of the optical fiber from the mirror was set to 2.5 mm; that was the distance above which no change in voltage output could be observed. Translating the stage and bringing the optical fiber closer to the mirror in steps of 0.1 mm and recording the voltage output the experimental curve of the voltage output against the distance was obtained. Using the non-linear least squares Gauss-Newton algorithm (Matlab - Curve Fitting Toolbox) the mathematical model (eq.5) was validated. The comparison with the experimantal data is shown in fig. 5; a maximum error of 4.8% was observed.

2) Lateral Force Loading

When applying lateral forces, the sensor tip part is tilted with regards to the Ƶ-axis and the angle between the upper part of the catheter and the main catheter shaft changes. As the deformable connecting link between the catheter shaft and tip accepts lateral forces the reflective surface rotates to an angle, Θ, in regards to its Ƶ-axis. This rotation changes the way the light is reflected back from the now angled reflecting surface diverting it away from the receiving optical fiber. The geometry of the intensity distribution profile for this case can be seen in fig. 6.

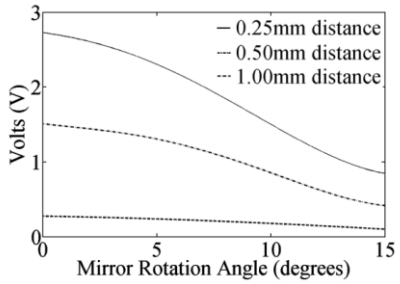

Fig. 7. Experimental data obtained rotating the mirror against the optical fiber in three different distances of 0.25, 0.5 and 1 mm.

An experiment was performed to determine the amount of light that can be detected by the photo detector when an optical fiber is placed in front of a rotating mirror. During the experiment the optical fiber was kept stationary and the mirror was positioned in front of the fiber's tip in such a way to be able to rotate left and right above the fiber. The experiment was conducted placing the mirror in 1 mm, 0.5 mm and 0.25 mm distance, respectively, from the optical fiber. For all three distances the mirror was rotated from 0° to 15° in increments of 1° step. The voltage output was recorded and the results are illustrated in fig. 7. From the graph, it can be observed that the sensitivity of the signal is affected by the distance between the mirror and the fiber; getting closer the mirror to the fiber, the greater the sensitivity. In addition, the voltage drop allows differentiating the axial from the lateral forces; the first yields a positive voltage signal while the second a negative one. That voltage drop increases when the angle of rotation increases.

C. Deformable Structure

In order to connect the catheter tip and the main catheter shaft a deformable structure was needed. That structure had to easily deform when accepting even the smallest of axial or lateral force and at the same time had to be MRI-compatible. For this system, the connecting structure was made out of a monolithic silicone rubber material with a hollow cylindrical slotted shape to avoid coupling effects and to maximize the deformations due to loading. The diameter of it is 12 Fr (4 mm) and its height 10 mm. Under axial loading the four symmetric vertical bars (the

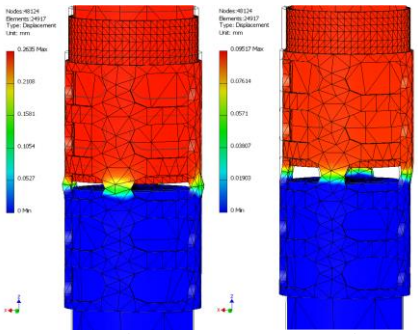

Fig. 8. The developed deformable structure in a deformation analysis using Finite Elements. Left: deformation of the structure in axial loading of the catheter tip. Right: deformation of the structure in lateral loading of the catheter tip.

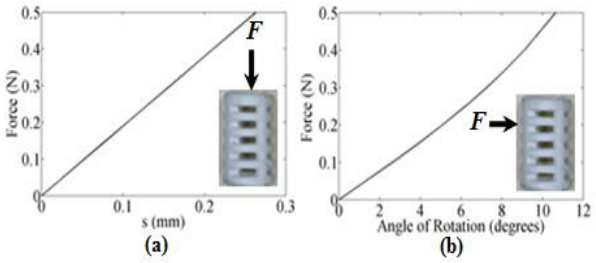

Fig. 9. (a) The simulated response of the deformable structure obtained by applying axial force from 0 to 0.5 N (~50 grams) and (b) The simulated response of the deformable structure obtained by applying lateral force from 0 to 0.5 N (~50 grams). The lateral deflection of the structure is shown in degrees.

connecting deformable parts of the catheter tip and the catheter shaft) are compressed equally minimizing the distance between optical fiber and reflective surface. On the other hand, during lateral loading, the bars are extended from the side where the force is applied and compressed at the other side rotating the reflective surface with respect to the fiber.

The deformable structure was simulated using stress analysis software techniques to determine the amount of deformation under various axial and lateral loadings, see fig. 8. Fig. 9 (a) and (b) show the simulation results indicating that under axial loads up to 0.5 N, the structure is linearly deforming with a maximum deformation of 0.28 mm. Under lateral loading, the structure rotates linearly as a function of the applied force by up to an angle of 8 degrees. It must be noted that the structure is able to withstand 1 N of force.

IV. Experiments

Experiments where performed to calibrate and test the performance of the sensor. Here a constant red light source with wavelength 650 nm, is used to transmit through a 0.25 mm optical fiber. The light bounces on the reflective surface and is collected back from the same optical fiber which is in turn connected to a fiber-optical coupler with 50:50 split ratio. Through the coupler the received light signal is guided to a photodiode detector, where it is transformed to a voltage signal. The voltage signal is then amplified and filtered for noise compensation by a dedicated amplifier circuitry. The amplified voltage output is send through a data acquisition card to a personal computer where the signal is further managed, observed and recorded using software techniques. The schematic representation of the entire system is shown in fig. 10.

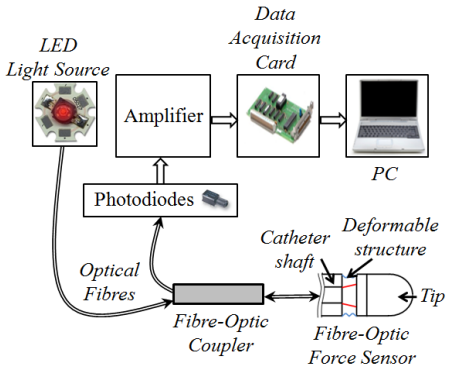

Fig. 10. Schematic diagram of operation of the miniaturized fiber-optic force sensor.

A. Loading-Unloading Cycle

The test rig for the calibration process consisted of the sensor, a rigid support to hold a linear translational stage in vertical position and an electronic scale. The developed sensor was mounted onto the linear stage vertically facing the electronic scale. The linear stage was able to move the catheter up and down in position; the sensor tip is force exerted onto the scale and was measured. Increased vertical displacement of the stage in negative direction corresponded into increased force exertion on the electronic scale. During the experiments the load on the sensor was increased in increments of 5 grams and the voltage output signal from the sensor was recorded. When 0.5 N of force was reached the linear stage moved back decreasing the load again in increments of 5 grams. The same protocol was applied laterally loading the sensor. This time a lateral force was applied to the tip of the sensor and measured by the scale. The experiments were repeated five times to verify the repeatability of the sensor. The sensor loading and unloading curves proved to be relative linear with small hysteresis, fig.11.

Under axial loading the sensor has a sensitivity of 1.9 N/V, a linear working range from 0 to 0.5 N and a resolution of 0.008 N. Under lateral loading it has an orientation dependent sensitivity possibly due to assembly misalignments; the sensor sensitivity varies from -3.0 V/N to -3.5 V/N depending on the side where the contact force is applied. The force working range is relatively linear from 0 to 0.5 N and the resolution is approximately -0.004 N.

B. Silicone Tests

In order to investigate the behaviour of the force sensor in surgery like environment further experiments were performed that simulates the motion of the catheter if moved by the hand of a physician.

During these experiments the catheter was attached to a slim rod. The developed sensor catheter tip was left to stand free 20 mm out of the rod's length while its other end was rigidly connected to a force sensor, ATI nano17 (ATI Industrial Automation, Inc., NC, USA). The aim was to compare the force output response of the developed force

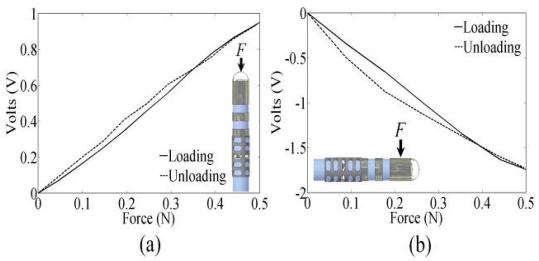

Fig. 11. Loading and Unloading axial (a) and lateral (b) cycles obtained after calibrating the force sensor.

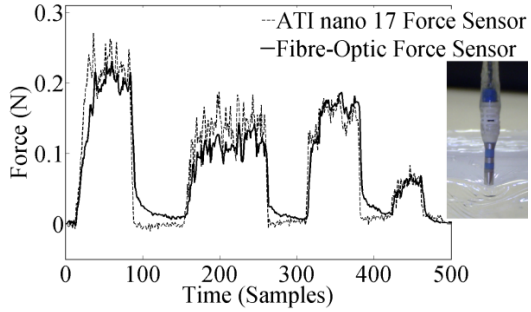

Fig. 12. Dynamic axial response of the force sensor when the catheter is pressed against a silicone block four times randomly by hand. The force results are compared with the response of a commercial force sensor. The hysteresis of the developed sensor that is caused by the rubber silicone material can be seen especially when a high force has stop been applied to it.

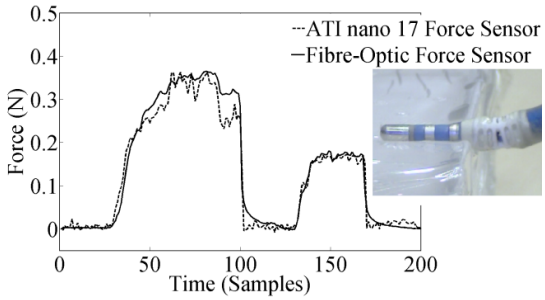

Fig. 13. Dynamic lateral response of the force sensor when the catheter is pressed against a silicone block two times randomly by hand. The force results are compared with the response of a commercial force sensor.

sensor against the force outputs of the force sensor whilst being subjected to the same dynamic loading and unloading conditions.

During a first experiment, fig.12, the developed sensor was held by a human vertically above a silicone block simulating the tissue properties of the heart. The catheter tip was moved to touch the silicone block several times to mimic the EP ablation procedure, where the physician touches the tissue and performs a burn. The force output signals from both sensors are shown in fig. 12. The experiment was repeated holding the catheter tip parallel to the surface of the silicone block to compare the lateral forces applied to both sensors; fig. 13.

These experiments show that the developed tip sensor can detect forces under axial and lateral loading and unloading conditions. The results of the developed fiber optic sensor matched the results of the commercial force sensor very well.

V. Conclusion

This paper reports on the preliminary findings of a miniature prototype force sensor that was developed and integrated with a 7 Fr EP ablation catheter to tackle the lack of force feedback that physicians encounter during cardio-vascular interventional procedures. The sensor employs a single optical fiber, a reflective surface and a deformable structure able to detect the interaction between axial or lateral forces of the catheter tip and tissue. Deformation of the sensor's structure modulates the light intensity making it possible to determine of the applied forces. The materials used for the development of the sensor make it MRI-compatible and thus safe for use inside MRI environments. Calibration and further experiments in soft tissue effigies returned satisfying results proving the feasibility of this low-cost, prototype force sensor. More detailed experiments, clinical trials and improvements are required. However, this paper shows that fiber optic sensors have the potential to be used in such minimally invasive procedures in the future.

Acknowledgment

The author's research studies are partially funded by the Alexander S. Onassis Public Benefit Foundation, which is based in Greece, and is greatly appreciated.

References

[1] F. WeiXing, W. HuanRan, G. ShuXiang, W. KeJun, Y. XiuFen, "Design and Experiments of a Catheter Side Wall Tactile Sensor for Minimum Invasive Surgery." *International Conference on Mechatronics and Automation*, pp.1073-1078, Harbin, 2007.

[2] P. Puangmali, K. Althoefer, L.D, Seneviratne, D. Murphy, P. Dasgupta, "State-of-the-Art in Force and Tactile Sensing for Minimally Invasive Surgery." *IEEE Sensors Journal*, Vol.8, (4), pp. 371-381, April 2008.

[3] V. Muthurangu, R. S. Razavi, "The value of magnetic resonance guided cardiaccatheterisation.", *Heart*, Vol. 91, pp. 995-996, 2005.

[4] R. Razavi, D.L.Hill, S.F. Keevil, M.E. Miquel, V. Muthurangu, S. Hegde, K. Rhode, M. Barnett, J. van Vaals, D.J. Hawkes, E. Baker, "Cardiac catheterisation guided by MRI in children and adults with congenital heart disease." *Lancet*, Vol. 362, pp.1877-82, 2003.

[5] N. Yu, R. Riener. "Review on MR-Compatible Robotic Systems." *The First IEEE/RAS-EMBS International Conference on Biomedical Robotics and Biomechatronics*, pp. 661-665, Pisa, Italy, 2006.

[6] R. Gassert, R. Moser, E. Burdet, H. Bleuler, "MRI/fMRI-Compatible Robotic System With ForceFeedback for Interaction With Human Motion", *IEEE/ASME Transactions on Mechatronics*, Vol. 11, no. 2, pp. 216-224,2006.

[7] T. Katsumata, Y. Haga,, K. Minami, M. Esashi. "Micromachined 125μm diameter ultra miniature fiber-optic pressure sensor for catheter." Transactions IEE Japan (Transactions IEE Japan) Vol. 120, no.2, pp. 58-63, 2000.

[8] H. Allen, K. Ramzan, J. Knutti, S. Withers, "A Novel Ultra-Miniature Catheter Tip Pressure Sensor Fabricated Using Silicon and Glass Thinning Techniques." *MRS Conference*, pp. I7.4, San Francisco, CA, 2001.

[9] D. Tanase, JFL. Goosen, P.J. Trimp, , PJ. French, "Multi-parameter sensor system with intravascular navigation for catheter/guide wire application." *Sensors and Actuators*, pp. 116-124, Germany, 2002.

[10] C. Strandman, L. Smithb, L. Tenerzb, B. Hök, "A production process of silicon sensor elements for a fiber-optic pressure sensor." *Sensors and Actuators*, Vol.63, no.1, pp.69-74, 1997.

[11] E. Cibula, D. Donlagic, C. Stropnik, "Miniature fiber optic pressure sensor for medical applications." *Proceedings of IEEE Sensors*, pp.711-714, 12-14 June 2002.

[12] K. Yokoyama, H. Nakagawa, D.C. Shah, H. Lambert, G. Leo, N. Aeby, A. Ikeda, J.V. Pitha, T. Sharma, R. Lazzara, W. M. Jackman. "Novel Contact Force Sensor Incorporated in Irrigated Radiofrequency Ablation Catheter Predicts Lesion Size and Incidence of Steam Pop and Thrombus." *Circulation: Arrhythmia and Electrophysiology*,Vol. 1, (5), pp. 354-362, December 2008.

[13] Panagiotis Polygerinos, Tobias Schaeffter, Lakmal D.Seneviratne, Kaspar Althoefer, "A Fiber-Optic Catheter-Tip Force Sensor with MRI Compatibility: A Feasibility Study", *IEEE Engineering in Medicine and Biology Conference*, Minneapolis, MN, USA, 2009.